0026-895X/09/7503-568–576$20.00
MOLECULAR PHARMACOLOGY
Copyright © 2009 The American Society for Pharmacology and Experimental Therapeutics
Mol Pharmacol 75:568–576, 2009

Vol. 75, No. 3
52589/3436665
Printed in U.S.A.

Analysis of DNA Methylation and Histone Modification Profiles of Liver-Specific Transporters[S]

Satoki Imai, Ryota Kikuchi, Hiroyuki Kusuhara, Shintaro Yagi, Kunio Shiota, and Yuichi Sugiyama

Department of Molecular Pharmacokinetics, Graduate School of Pharmaceutical Sciences, the University of Tokyo, Tokyo, Japan (S.I., R.K., H.K., Y.S.); and Laboratory of Cellular Biochemistry, Department of Animal Resource Sciences/Veterinary Medical Sciences, the University of Tokyo, Tokyo, Japan (S.Y., K.S.)

Received October 7, 2008; accepted December 1, 2008

ABSTRACT

Tissue-specific expression of transporters is tightly linked with their physiological functions through the regulation of the membrane transport of their substrates. We hypothesized that epigenetic regulation underlies the tissue-specific expression of mouse liver-specific transporters (*Oatp1b2*/*Slco1b2*, *Ntcp*/*Slc10a1*, *Bsep*/*Abcb11*, and *Abcg5*/*g8*). We examined their DNA methylation and histone modification profiles near the transcriptional start site (TSS) in the liver, kidney, and cerebrum. Genome-wide DNA methylation profiling with tissue-dependent differentially methylated region profiling with restriction tag-mediated amplification and subsequent bisulfite genomic sequencing demonstrated that the CpG dinucleotides around the TSS of *Oatp1b2* (from −515 to +149 CpGs), *Ntcp* (from −481 to +495 CpGs), *Bsep* (from −339 to +282 CpGs), and *Abcg5*/*g8* (from −161 to +5 CpGs for *Abcg5*, i.e., from −213 to −48 CpGs for *Abcg8*) were hypomethylated in the liver and hypermethylated in the kidney and cerebrum. The opposite pattern was observed for *Pept2*/*Slc15a2* (from −638 to +4 CpGs), which was expressed in the kidney and cerebrum but not in the liver. These DNA methylation profiles are consistent with the tissue distribution of these transporters. A chromatin immunoprecipitation assay demonstrated that the histone H3 associated with *Oatp1b2*, *Ntcp*, *Bsep*, and *Abcg5*/*g8* promoters was hyperacetylated in the liver but was acetylated very little in the kidney and cerebrum, whereas the upstream region of *Pept2* was hyperacetylated only in the kidney and cerebrum. These results suggest the involvement of epigenetic systems in the tissue-specific expression of mouse transporters *Oatp1b2*, *Ntcp*, *Bsep*, *Abcg5*/*g8*, and *Pept2*.

During the past two decades, extensive research has sought to uncover the molecular characteristics of transporters to explain their physiological and pathological functions. These transporters comprise more than 300 genes that are now classified into the solute carrier (SLC) and ATP-binding cassette (ABC) transporter superfamilies. Transporters show tissue-specific expression patterns that have critical implications for the physiological function of certain tissues (Borst and Elferink, 2002; Kusuhara and Sugiyama, 2002; Hediger et al., 2004; Stefkova et al., 2004; Shitara et al., 2006).

Liver tissue is one of the most important tissues in terms of the physiological turnover of endogenous compounds, such as bile acids and sterols, and the clearance of exogenous substances, including clinically used drugs. Several transporters are closely related to the hepatobiliary transport of these compounds. SLC-type transporters mediate the hepatic uptake of bile acids and xenobiotic organic anions, and ABC transporters then contribute to the biliary efflux of bile acids, sterols, and xenobiotic compounds and their metabolites (Faber et al., 2003; Chandra and Brouwer, 2004). Numerous reports suggest the involvement of liver-enriched transcription factors, such as hepatocyte nuclear factors (HNFs) 1, 3, and 4, and proteins of the CCAAT/enhancer-binding protein family, in the transcriptional regulation of liver-specific genes (Cereghini, 1996). However, these transcription factors are not expressed exclusively in the liver but are also observed in other tissues, implying that other machineries cooperate with the transcription factor network to establish and maintain the liver-specific gene expression pattern.

Article, publication date, and citation information can be found at http://molpharm.aspetjournals.org.
doi:10.1124/mol.108.052589.
[S] The online version of this article (available at http://molpharm.aspetjournals.org) contains supplemental material.

ABBREVIATIONS: SLC, solute carrier; ABC, ATP binding cassette; Bsep, bile salt export pump; ChIP, chromatin immunoprecipitation; D-REAM, tissue-dependent differentially methylated region profiling with restriction tag-mediated amplification; HNF, hepatocyte nuclear factor; Ntcp, Na^+-taurocholate-cotransporting polypeptide; Oatp, organic anion transporting polypeptide; PCR, polymerase chain reaction; RT-PCR, reverse transcription polymerase chain reaction; Pept2, peptide transporter 2; T-DMR, tissue-dependent differentially methylated region; T-DMRtag, tag of the tissue-dependent differentially methylated region; TSS, transcriptional start site.

The role of epigenetic systems comprising DNA methylation and histone modification has attracted much interest as a possible mechanism underlying the tissue-specific gene expression (Bird, 2002; Shiota, 2004; Ohgane et al., 2008). Methylation of CpG dinucleotides, the unique target of DNA methylation in vertebrates, can evoke the condensed structure of chromatin by recruiting chromatin-remodeling factors, such as methyl CpG-binding proteins and histone deacetylases, and can prevent the transactivation of neighboring genes by most of the transcription factors. Therefore, gene expression is inversely correlated with DNA methylation in the 5′-flanking region. Our research group and other groups have demonstrated the involvement of DNA methylation-mediated gene silencing in the kidney-specific expression of SLC transporters, including the human organic anion transporter 3/*SLC22A8*, mouse urate transporter 1/*Slc22a12*, and human organic cation transporter 2/*SLC22A2* (Kikuchi et al., 2006, 2007; Aoki et al., 2008). The DNA methylation status affects the accessibility of HNF1α/β to the recognition sequence within the promoter and confers the tissue-specificity of organic anion transporter 3 and urate transporter 1, whereas organic cation transporter 2 requires upstream stimulating factor 1 as a downstream transcription factor. The role of epigenetic regulation in the expression of liver-specific transporters has not been investigated.

We recently established a novel method, tissue-dependent differentially methylated region (T-DMR) profiling with restriction tag-mediated amplification (D-REAM) (Yagi et al., 2008), for analyzing the DNA methylation profiles of gene promoters that include HpyCH4IV restriction sites on a genome-wide scale. Plurality of the T-DMRs identified in D-REAM is associated with the tissue-specific expression of the neighboring genes in the liver. The aim of the present study was to explore systematically the contribution of epigenetic regulation to the liver-specific expression of transporters. We used D-REAM to investigate the DNA methylation status in the 5′-flanking region of almost all mouse SLC and ABC transporter genes in the liver, kidney, and cerebrum and found that the liver-specific transporters, organic anion transporting polypeptide 1b2 (Oatp1b2)/*Slco1b2*, Na^+-taurocholate-cotransporting polypeptide (Ntcp)/*Slc10a1*, bile salt export pump (Bsep)/*Abcb11*, *Abcg5*, and *Abcg8*, possess T-DMRs hypomethylated in the liver. Oatp1b2 and Ntcp mediate the sodium-independent and -dependent uptake of amphipathic organic anions and bile acids, respectively (Wolkoff and Cohen, 2003; Evers and Chu, 2008). Bsep is an ABC transporter that plays a pivotal role in the canalicular efflux of bile acids (Trauner and Boyer, 2003). Abcg5 and Abcg8 form a heterodimer to function as an efflux transporter for sterols into the bile (Hazard and Patel, 2007; Kidambi and Patel, 2008). The genes for BSEP and ABCG5/G8 are those responsible for the hereditary disorders progressive familial intrahepatic cholestasis type 2 (Strautnieks et al., 1998) and sitosterolemia (Berge et al., 2000; Lee et al., 2001; Lu et al., 2001), respectively. Bisulfite genomic sequencing and a chromatin immunoprecipitation (ChIP) assay were used to confirm and examine more extensively the DNA methylation and histone H3 acetylation profiles, respectively. Here we provide clear evidence that the liver-specific expression of mouse Oatp1b2, Ntcp, Bsep, Abcg5, and Abcg8 is associated with DNA methylation and histone acetylation in their promoters.

Materials and Methods

Materials. All reagents were purchased from Wako Pure Chemicals (Osaka, Japan) unless stated otherwise.

D-REAM. D-REAM and subsequent bioinformatics analysis were carried out as described previously for genomic DNA from the liver, kidney, and cerebrum of C57BL/6NCrj male mice at 12 or 13 weeks of age (Yagi et al., 2008). In brief, the genomic DNA was digested with a methylation-sensitive restriction enzyme HpyCH4IV that recognizes ACGT residues followed by subsequent amplification by modified ligation-mediated polymerase chain reaction (PCR). Because only the unmethylated DNA is digested by HpyCH4IV, the modified ligation-mediated PCR facilitates the selective amplification of the unmethylated region in the genomic DNA. The amplified fragments were then hybridized with mouse promoter tiling array, and the array signal intensities were analyzed to identify regions corresponding to fragments in unmethylated HpyCH4IV sites. Comparison of signals from different samples enabled the identification of differentially methylated regions. Genomic annotations, including Ensembl gene assignments, were performed on the Galaxy website (available at http://main.g2.bx.psu.edu/). The analyzed data were then visualized with the Integrated Genome Browser (available at http://www.affymetrix.com/partners_programs/programs/developer/tools/download_igb.affx). Tags of T-DMR (T-DMRtags) in the liver, kidney, and cerebrum were defined as the HpyCH4IV sites that are hypomethylated in the liver, kidney, and cerebrum compared with other tissues, respectively.

Genomic DNA Extraction and Bisulfite Reaction. Genomic DNA was extracted from the liver, kidney, and cerebrum of 11-week-old male C57BL/6NCrj mice using a Get Pure DNA Kit (Dojindo Molecular Technologies, Gaithersburg, MD) according to the manufacturer's instructions. Five to 10 μg of genomic DNA was digested with EcoRI and subjected to the bisulfite reaction as described previously (Kikuchi et al., 2007). The DNA was then precipitated with ethanol, dried, and resuspended in buffer containing 10 mM Tris-HCl and 1 mM EDTA, pH 8.0.

Combined Bisulfite Restriction Analysis. The DNA fragments encompassing the T-DMRtags of *Oatp1b2*/*Slco1b2*, *Ntcp*/*Slc10a1*, *Bsep*/*Abcb11*, *Abcg5*, and *Pept2*/*Slc15a2* were amplified by PCR using the following primers: *Oatp1b2* −594 (forward) to −347 (reverse); *Ntcp* +179 (forward) to + 671 (reverse); *Bsep* −110 (forward) to +416 (reverse); *Abcg5* +1035 (forward) to +1212 (reverse); and *Pept2* −171 (forward) to +155 (reverse) (Table 1). PCR was performed using Immolace DNA Polymerase (Bioline, London, UK) under the following conditions: 94°C for 10 min; 43 cycles of 94°C for 30 s, 53°C (*Oatp1b2* and *Pept2*) or 55°C (*Ntcp*, *Bsep*, and *Abcg5*) for 30 s, and 72°C for 1 min; and final extension of 72°C for 10 min. The PCR fragments were digested with HpyCH4IV (New England Biolabs, Ipswich, MA) to confirm the methylation status of the T-DMRtags. Because only unmethylated cytosine residues are changed to thymines by the bisulfite reaction, PCR fragments from unmethylated genomic DNA are resistant to HpyCH4IV digestion, whereas those from methylated DNA are digested. The resultant products were electrophoresed on a 2.0% agarose gel and stained with ethidium bromide.

Bisulfite Genomic Sequencing. The DNA fragments covering the genomic region around the TSS of SLC or ABC transporters were amplified by PCR using the following primers: *Oatp1b2*, −594 (forward) to −347 (reverse) or −40 (forward) to +208 (reverse); *Ntcp*, −542 (forward) to −1 (reverse) or −46 (forward) to +522 (reverse); *Bsep*, −404 (forward) to −90 (reverse) or −110 (forward) to +340 (reverse); *Abcg5*, −315 (forward) to +125 (reverse); and *Pept2*, −669 (forward) to −144 (reverse) or −171 (forward) to +155 (reverse) (Table 1). The PCR was performed under the following conditions: 94°C for 10 min; 43 cycles of 94°C for 30 s, 53°C [*Oatp1b2*, −594 (forward)/−347 (reverse) and *Pept2*, −171 (forward)/+155 (reverse)], 55°C [*Oatp1b2*, −40 (forward)/+208 (reverse); *Ntcp*, −46 (forward)/+522 (reverse); *Bsep*, −404 (forward)/−90 (reverse); *Bsep*, −110

TABLE 1
Oligonucleotides used for the combined bisulfite restriction analysis, bisulfite PCR, RT-PCR, and real-time PCR in the ChIP assay
Positions of primers for the RT-PCR are based on the published cDNA sequences, whereas those for the other experiments are relative to the TSS in the genome.

Oligonucleotide and Orientation	Sequence (5′ to 3′)	Position
Primers used for the combined bisulfite restriction analysis and the bisulfite PCR		
Oatp1b2		
−594-F	GGTTATTTGATTTTTGATAAAGGAGT	−594 to −569
−347-R	TACCCACTACTTAAAAACATTCAATA	−347 to −372
−40-F	GTAGAGAGGTTTTAAAGTGGGAT	−40 to −18
+208-R	ACCTAAACCACATCTATCTCCTA	+208 to +186
Ntcp		
−542-F	GTAAGGTTTTAGAGGAGGAT	−542 to −523
−1-R	CCTTCCTTACCCAATACTAA	−1 to −20
−46-F	GAAAGAGGATTGAAGAAAAT	−46 to −20
+522-R	CAATACCAAACTTAATCCAA	+522 to +503
+179-F	GAGTTTAGTAAGATTAAGGT	+179 to +198
+671-R	TCTCCTTTACAATAATCCTA	+671 to +652
Bsep		
−404-F	GGTTTTAGATTATTGAGGGTTTGT	−404 to −381
−90-R	CCTAAAATCCAAATCTAACACAATTCAA	−90 to −117
−110-F	GTGTTAGATTTGGATTTTAGGTT	−110 to −88
+340-R	ACACACACACACACATTTTTAAA	+340 to +318
+416-R	CCAAATTTAAAAAACATCTCTCTA	+416 to +393
Abcg5		
−315-F	TAGTTATGATTAGTGTTGTTTGTGT	−315 to −291
+125-R	CAAAAAACTCAAAAACCCTCTATTA	+125 to +100
+1035-F	GGTATTTGAATATAATTTGGTGAT	+1035 to +1058
+1212-R	TAAACATACCCAAAACTCTA	+1212 to +1193
Pept2		
−669-F	GTTGAATGTTATGATGTTGAAAATT	−669 to −645
−144-R	TACAACATCTTAACTAAACATACAA	−144 to −168
−171-F	GAGTTGTATGTTTAGTTAAGATGTTGT	−171 to −145
+155-R	AACTAAAACTACTACCAACCTACAATA	+155 to +129
Primers used for the RT-PCR		
Oatp1b2		
Forward	GGAGGGTGCAGAGCTAGATG	+471 to +490
Reverse	ATTCCTCGAGATCCCCTTGT	+671 to +652
Ntcp		
Forward	GTTTAAATCCCAGGGGGAAA	+571 to +590
Reverse	CGTTTGGTTCCAAGTCACCT	+807 to +788
Bsep		
Forward	AGCTTCCGTTGTTCTCAGGA	+496 to +515
Reverse	GGTGGAGAGGAGGGAAGAAC	+684 to +665
Abcg5		
Forward	TGGTGGCCAACTTGTCATTA	+622 to +641
Reverse	CAAGGGCAAAGGCAGAGTAG	+774 to +755
Abcg8		
Forward	TTGGCATTGTTTGGTGAGAA	+524 to +543
Reverse	AAGGTAGCGAGATGCCTCAA	+696 to +677
Pept2		
Forward	TGAGTCCAAGGAAACGCTCT	+224 to +243
Reverse	CCAACAGCCAACGAGAAACT	+384 to +365
β-actin		
Forward	CAGCCAACTTTACGCCTAGC	+208 to +227
Reverse	GGTTTGGACAAAGACCCAGA	+453 to +434
Primers used for the real-time PCR in ChIP assay		
Oatp1b2		
Forward	TTGTGTAGGACAGTGACCTGAAG	−94 to −72
Reverse	GGCATGTCTAACCTGCACCT	+12 to −8
Ntcp		
Forward	ATCCGGGGAGATGAGGTTAT	−154 to −135
Reverse	CCACCTCACTCTCTGCTCCT	+22 to +3
Bsep		
Forward	TTTGGGTTCCTGCTTTGAGT	−162 to −143
Reverse	GGTTGTACACCCCTTTCCAA	+12 to −8
Abcg5		
Forward	TCCTCTCTGGCAAACACTCC	−192 to −173
Reverse	CAGGGCAGCTTTAACTGAGG	−1 to −20
Pept2		
Forward	TCTGAAATCAGCCTTCTGTGTT	−278 to −257
Reverse	CACGTCACAAGTCACGAGATG	−38 to −58
β-actin		
Forward	AAATGCTGCACTGTGCGGCG	−139 to −120
Reverse	AGGCAACTTTCGGAACGGCG	−63 to −82

F, forward; R, reverse.

(forward)/+340 (reverse); and *Abcg5*, −315 (forward)/+125 (reverse)], or 57°C [*Ntcp*, −542 (forward)/−1 (reverse) and *Pept2*, −669 (forward)/−144 (reverse)] for 30 s, and 72°C for 1 min; and final extension of 72°C for 10 min. The PCR products were cloned into the pGEM-T Easy vector (Promega, Madison, WI), and 10 clones chosen randomly from each sample were sequenced to determine the presence of methylated cytosines.

RNA Isolation and RT-PCR. Total RNA was isolated from the liver, kidney, and cerebrum of a 14-week-old male C57BL/6NCrj mouse using ISOGEN (Nippon Gene, Toyama, Japan) according to the manufacturer's instructions. The RNA was then treated with DNase I to remove the contaminated genomic DNA, followed by reverse transcription using a random nonamer primer (Takara, Shiga, Japan). PCR was performed with the forward and reverse primers listed in Table 1 to detect the partial fragments of Oatp1b2, Ntcp, Bsep, Abcg5, Abcg8, Pept2, and *β-actin* cDNA. PCR was performed under the following conditions: 94°C for 2 min; 30 cycles (Oatp1b2, Bsep, and Abcg8), 32 cycles (Ntcp, Abcg5, and Pept2), or 35 cycles (β-actin) of 94°C for 30 s, 55°C for 30 s, and 72°C for 1 min; and final extension of 72°C for 5 min. The resultant products were electrophoresed on a 2.0% agarose gel and stained with ethidium bromide.

ChIP Assay. The ChIP assay was performed using antiacetylated histone H3 antibody (Millipore, Billerica, MA) according to a procedure described previously (Fujii et al., 2006) and the Farnham Laboratory's protocol (available at http://www.genomecenter.ucdavis.edu/farnham/protocols/tissues.html) with minor modifications. Normal rabbit IgG was used as a negative control to verify the immunoprecipitation specificity. In brief, approximately 250 mg of tissue was chopped into small pieces and treated with 1% formaldehyde to form DNA-protein cross-links. The samples were homogenized, treated with cell lysis buffer, and centrifuged to precipitate the nuclei. The nuclei were then lysed with nuclei lysis buffer and sonicated on ice. The samples were preincubated with salmon sperm DNA/protein A-agarose suspension to reduce the nonspecific background, and the samples were incubated with an antibody against acetylated histone H3, normal rabbit IgG, or an equivalent amount of phosphate-buffered saline as the "no antibody" sample at 4°C overnight. The samples were then mixed with salmon sperm DNA/protein A-agarose suspension, rotated for 60 min at 4°C, and centrifuged at 20,000*g* for 1 min at 4°C. DNA was purified from the precipitated immune complex after extensive washing and reversing of the DNA-protein cross-links. The supernatant from the "no antibody" sample was collected as the "total input". The quantitative real-time PCR was performed using a LightCycler and the appropriate software (version 3; Roche Diagnostics, Indianapolis, IN) according to the manufacturer's instructions with the primers shown in Table 1. The protocol for PCR was as follows: 95°C for 30 s, and then 40 cycles of 95°C for 5 s, 58°C for 10 s, and 72°C for 15 s. The enrichment of DNA in the immunoprecipitates was calculated relative to the 1:100 diluted "total input" samples.

Results

Screening of T-DMRtags by D-REAM. Screening with D-REAM revealed that 53 of 297 SLC transporter genes and 11 of 49 ABC transporter genes were associated with T-DMRtags that were hypomethylated in the liver and hypermethylated in the kidney or cerebrum in the genomic region from −6.0 to +2.5 kilobase pairs around the TSS (Supplemental Table 1). We focused on *Oatp1b2*/*Slco1b2*, *Ntcp*/*Slc10a1*, *Bsep*/*Abcb11*, *Abcg5*, and *Abcg8*, which are expressed predominantly in the liver, where they play indispensable roles in the hepatobiliary transport of endogenous and exogenous substances. D-REAM also located the T-DMRtag hypomethylated in the kidney and cerebrum whereas it was hypermethylated in the liver in the 5′-flanking region of *Pept2*, which is expressed predominantly in the kidney and cerebrum.

Combined Bisulfite Restriction Analysis of T-DMR Tags in SLC and ABC Transporters. Integrated Genome Browser plots of comparative D-REAM signals are shown around the TSS of *Oatp1b2*, *Ntcp*, *Bsep*, *Abcg5*, *Abcg8*, and *Pept2* (Fig. 1A). These data suggest that the CpG dinucleotides at −515, +495, +224, +1141, and +1405 or +1431 base pairs relative to the TSS of *Oatp1b2*, *Ntcp*, *Bsep*, *Abcg5*, and *Abcg8*, respectively, are hypomethylated in the liver, whereas these sites are hypermethylated in the kidney and cerebrum. The CpG dinucleotide located at −41 base pairs relative to the TSS of *Pept2* is hypomethylated in the kidney and cerebrum, whereas this site is hypermethylated in the liver. The DNA methylation status of these T-DMRtags found by D-REAM was verified in vivo in a combined bisulfite restriction analysis using HpyCH4IV as the restriction enzyme (Fig. 1B). These analyses corroborated that the T-DMRtags in *Oatp1b2*, *Ntcp*, *Bsep*, and *Abcg5* genes are hypomethylated in the liver but hypermethylated in the kidney and cerebrum and vice versa for *Pept2*. The genomic region around the T-DMRtag in *Abcg8* gene was not amplified after extensive PCR, and it was not possible to validate the D-REAM data with combined bisulfite restriction analysis (data not shown).

mRNA Expression Profiles of the SLC and ABC Transporters. The mRNA expression of Oatp1b2, Ntcp, Bsep, Abcg5, Abcg8, and Pept2 in the mouse liver, kidney, and cerebrum was investigated by RT-PCR (Fig. 2). The results confirmed the liver-specific expression of Oatp1b2, Ntcp, Bsep, Abcg5, and Abcg8. The expression of Pept2 was significant in both the kidney and cerebrum but was negligible in the liver.

DNA Methylation Profiles around the Transcriptional Start Site. The DNA methylation profiles in the CpG dinucleotides around the TSS of the above-mentioned transporters in mouse liver, kidney, and cerebrum were determined by bisulfite genomic sequencing (Fig. 3, A–E). The CpG dinucleotides around the TSS of *Oatp1b2*, *Ntcp*, and *Bsep* were overall significantly hypomethylated in the liver compared with the kidney and cerebrum (Fig. 3, A–C). The CpGs inside or adjacent to the intergenic region of *Abcg5* and *Abcg8* were also hypomethylated considerably in the liver but were hypermethylated in the kidney and cerebrum (Fig. 3D). The DNA methylation profiles are consistent with the liver-specific expression of the corresponding transporters. In contrast, the bisulfite sequencing for *Pept2* demonstrated that the genomic region is hypomethylated in the kidney and cerebrum but hypermethylated in the liver, especially in the CpG dinucleotides located at −527, −54, −41, and +4 relative to the TSS, which is consistent with the predominant expression of this transporter in the kidney and cerebrum (Fig. 3E). These results suggest that the regions around the TSS of *Oatp1b2*, *Ntcp*, *Bsep*, and *Abcg5*/*g8* can be regarded as T-DMRs and that the tissue-specific expression of these transporters is regulated through DNA methylation-mediated gene silencing.

Histone Acetylation Profiles in the Promoter Region. It is generally recognized that the DNA methylation status is linked tightly with the histone acetylation status and that activated genes are associated with acetylated histone H3. Thus, we performed ChIP assays to examine further the histone H3 acetylation profiles of the transporter genes

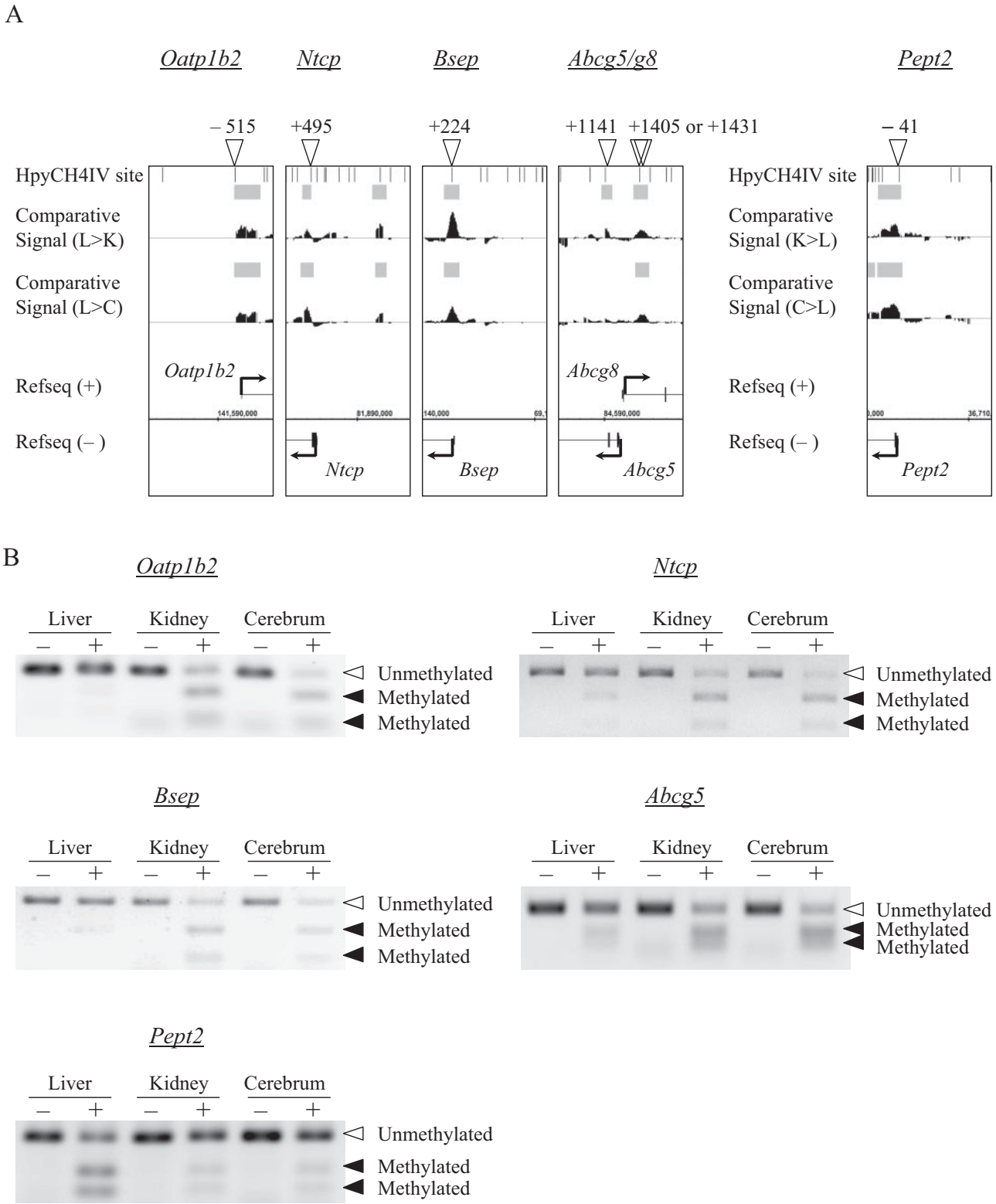

Fig. 1. Comparative D-REAM and combined bisulfite restriction analysis. A, Integrated Genome Browser plots of comparative D-REAM signals. D-REAM and subsequent bioinformatics analysis were carried out and the analyzed data for *Oatp1b2*, *Ntcp*, *Bsep*, *Abcg5/g8*, and *Pept2* were visualized with Integrated Genome Browser. Arrowheads and vertical bars represent T-DMRtags and HpyCH4IV sites, respectively. Comparative signals between tissues and significantly different regions are indicated as plots and gray bars, respectively. L, liver; K, kidney; C, cerebrum. B, combined bisulfite restriction analysis of T-DMRtags. The bisulfite PCR products were digested with HpyCH4IV and electrophoresed on a 2.0% agarose gel to evaluate the methylation status of T-DMRtags. The conditions of undigested (−) and digested (+) are indicated on the top of the gel. Because only unmethylated cytosine residues are converted to thymines by the bisulfite reaction, PCR fragments from unmethylated genomic DNA are resistant to HpyCH4IV digestion, whereas fragments from methylated DNA are digested. The representative image of at least two independent experiments is shown.

with T-DMRs. In the liver, histone H3 in the proximal promoter of *Oatp1b2*, *Ntcp*, *Bsep*, and *Abcg5/g8* was hyperacetylated, whereas the acetylation in the kidney and the cerebrum was minimal (Fig. 4). In contrast, acetylated histone H3 for the *Pept2* upstream region was observed in the kidney and cerebrum but not in the liver. Histone H3 in the *β-actin* promoter was hyperacetylated in all tissues. These in vivo histone acetylation profiles were compatible with the tissue-specific expression of the transporter genes.

Discussion

The expression of transporters is an important determinant of the physiological functions of liver and kidney, including the efficient turnover of endogenous compounds and elimination of xenobiotics. Although the involvement of epigenetic machineries in the kidney-specific expression of transporters has emerged, those in the liver-specific transporters have not been investigated. We examined comprehensively the epigenetic signatures of SLC and ABC transporters in mice, focusing particularly on those expressed exclusively in the liver.

Analysis with D-REAM and subsequent bisulfite genomic sequencing located T-DMRs that are hypomethylated in the liver but hypermethylated in the kidney or cerebrum over a wide range of genomic regions around the TSS of liver-specific transporters (Figs. 1 and 3). The histone H3 acetylation profiles neighboring the TSS also coincided with the tissue-specific expression of these transporters (Fig. 4). These results strongly suggest that the constitutive expression of liver-specific transporters involves the epigenetic signatures comprising DNA methylation and chromatin modification. Together with our previous findings (Kikuchi et al., 2006, 2007) and our ongoing study of the kidney-specific transporters (R. Kikuchi, S. Yagi, H. Kusuhara, Y. Sugiyama, K. Shiota, unpublished observations), the epigenetic regulation should be prevalent among transporters expressed in the liver and kidney.

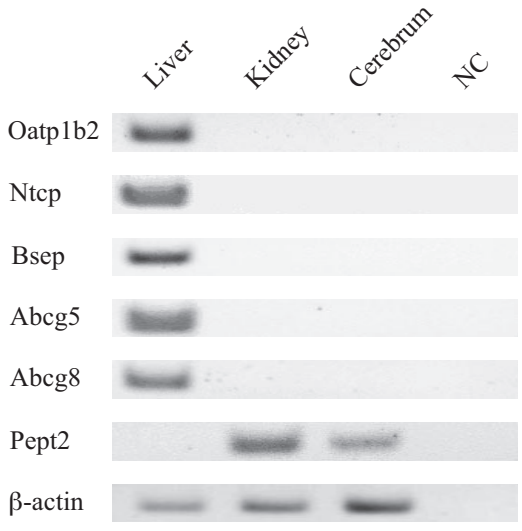

Fig. 2. mRNA expression profiles of the SLC and ABC transporters. mRNA expression of Oatp1b2, Ntcp, Bsep, Abcg5, Abcg8, Pept2, and β-actin in mouse liver, kidney, and cerebrum was determined by RT-PCR using specific primers (Table 1) as described under *Materials and Methods*. An equal amount of total RNA was used for each sample, and distilled water was included as a negative control (NC). The identity of the PCR products is shown on the left.

Promoter analysis of liver-specific transporters has unveiled the involvement of several transcription factors in mice, including HNF1α (Jung et al., 2001; Maher et al., 2006), glucocorticoid receptor (Eloranta et al., 2006), farnesoid X receptor (Sinal et al., 2000; Ananthanarayanan et al., 2001; Plass et al., 2002), and HNF4α (Sumi et al., 2007), which are responsible for the promoter activation of *Oatp1b2*, *Ntcp*, *Bsep*, and *Abcg5/g8*, respectively. According to the computational analysis with MatInspector (available at http://www.genomatix.de/), the position of the potential transcription factor binding motifs relative to the TSS of each transporter is as follows: HNF1-motif in *Oatp1b2* promoter, −67 to −51; glucocorticoid response element in *Ntcp* promoter, −65 to −47; farnesoid X receptor response element in *Bsep* promoter, −92 to −80; and HNF4α-motif (DR-1 motif) in *Abcg5/g8* intergenic region, −126 to −114 relative to the TSS of *Abcg5* (−94 to −82 relative to the TSS of *Abcg8*). These binding motifs do not contain CpG dinucleotides but are surrounded by differentially methylated CpG dinucleotides in different tissues. Together with the different histone acetylation profiles in various tissues, it is likely that DNA methylation interrupts the binding of transcription factors indirectly through the recruitment of histone deacetylases and the subsequent chromatin condensation (Fig. 5).

It is interesting that our data emphasize that epigenetic regulation underlies the liver-specific expression of functionally cooperated transporters. Ntcp and Bsep are responsible for the sinusoidal uptake and canalicular efflux of bile acids in hepatocytes, respectively (Trauner and Boyer, 2003; Mita et al., 2006; Alrefai and Gill, 2007). Simultaneous liver-specific expression of these transporters is indispensable for the vectorial transport of bile acids under physiological conditions. Likewise, Abcg5 and Abcg8 form a heterodimer to function as the efflux transporter for sitosterols and cholesterols in the liver and to prevent the intestinal absorption of sitosterols (Hazard and Patel, 2007; Kidambi and Patel, 2008). The genes for these transporters are located in close proximity but with opposite orientation in the genome in both the human and mouse, and the intergenic region in human homologs has bidirectional promoter activity. The common regulatory mechanism, including the epigenetic traits and probably transcription factors, should lead to the same tissue distribution pattern of these two sets of functionally paired transporters.

It is noteworthy that members of the Oatp family, such as *Oatp1a1*, *Oatp1a4*, *Oatp1a5*, *Oatp1a6*, *Oatp1b2*, and *Oatp1c1*, exist in tandem on the same chromosome (Hagenbuch and Meier, 2004). Oatp1a1, Oatp1a4, Oatp1a5, and Oatp1a6 show particularly high sequence homology at the amino acid level to each other (>70%) and also show moderate sequence homology to Oatp1b2 and Oatp1c1 (>40%) (Hagenbuch and Meier, 2003), indicating that these isoforms are products of genetic duplication from the same ancestor gene. These Oatp isoforms show overlapping substrate specificities and are functionally redundant, except for Oatp1c1, which is relatively specific for thyroid hormone (Tohyama et al., 2004). Each member exhibits a unique tissue distribution (e.g., Oatp1a1 is expressed predominantly in the liver and kidney; Oatp1a4 and Oatp1a5 are expressed in the liver, kidney, and cerebrum; and Oatp1b2, Oatp1a6, and Oatp1c1 are expressed exclusively in the liver,

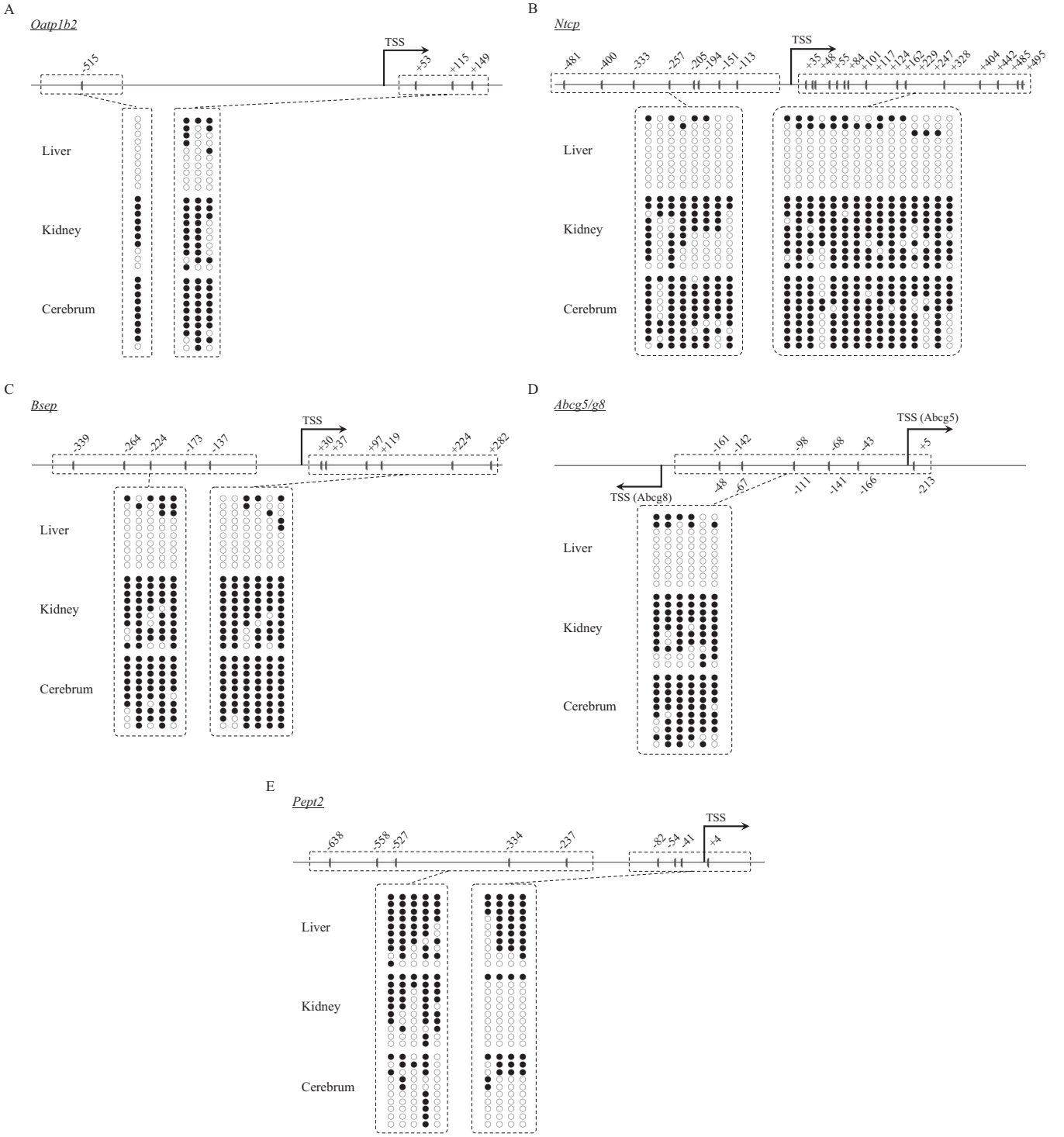

Fig. 3. DNA methylation profiles around the transcriptional start site. Bisulfite genomic sequencing analysis was performed for *Oatp1b2* (A), *Ntcp* (B), *Bsep* (C), *Abcg5/g8* (D), and *Pept2* (E) with genomic DNA extracted from mouse liver, kidney, and cerebrum as described under *Materials and Methods*. Top, a schematic diagram of the genomic region around the TSS. The vertical lines and numbers indicate the positions of the cytosine residues of the CpG dinucleotides relative to the TSS (+1). Bottom, DNA methylation status of individual CpG dinucleotides. The open and closed circles represent unmethylated and methylated cytosines, respectively.

kidney, and cerebrum, respectively). The liver-specific expression of Oatp1b2 is associated with its epigenetic signature, indicating that the difference in the epigenetic signature distinguishes each isoform of the Oatp family transporters in terms of its tissue distribution, thus conferring functional diversity from the same ancestor gene during the evolutional process. Future studies should show the in vivo relevance of epigenetic regulation for other Oatp transporters.

In conclusion, our study revealed strong associations between the liver-specific expression and epigenetic profiles comprising DNA methylation and histone acetylation for *Oatp1b2*, *Ntcp*, *Bsep*, and *Abcg5/g8* in mice. Together with our previous findings on the kidney-specific transporters, it is plausible that epigenetic regulation is a mechanism with considerable universality that underlies the tissue-specific expression of SLC and ABC transporters.

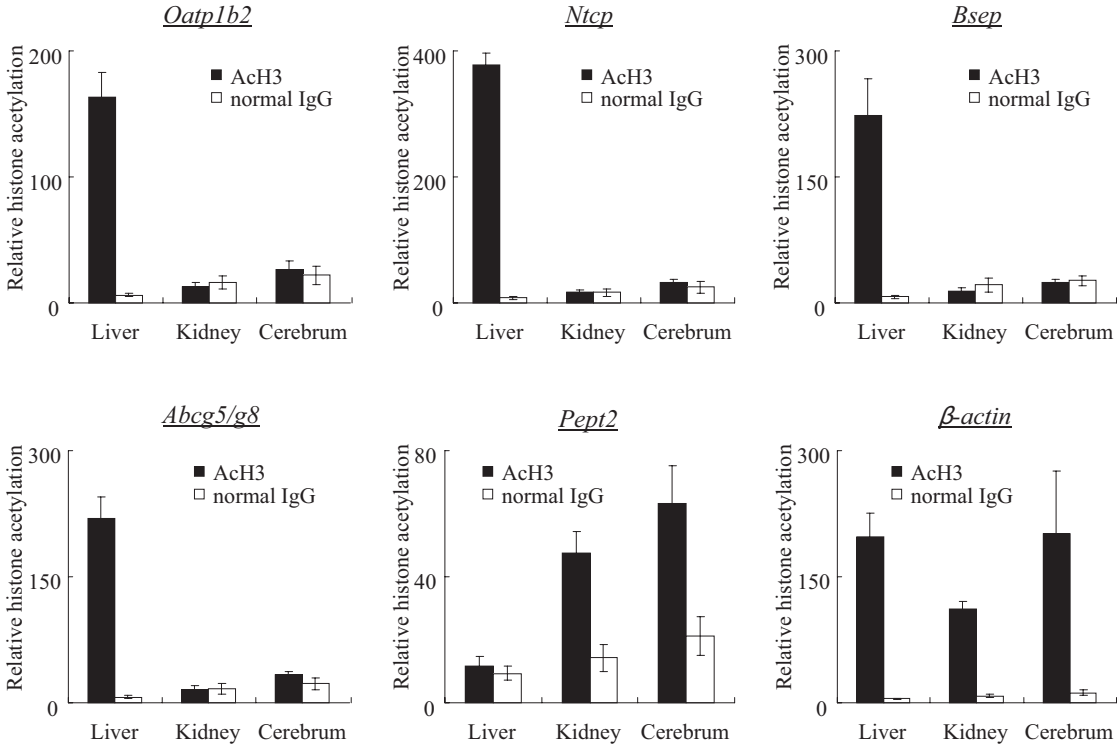

Fig. 4. Histone acetylation profiles in the promoter region. The histone H3 acetylation status of *Oatp1b2*, *Ntcp*, *Bsep*, *Abcg5/g8*, *Pept2*, and *β-actin* in the promoter region was determined by ChIP assay in mouse liver, kidney, and cerebrum as described under *Materials and Methods*. The closed columns represent the histone acetylation of each sample relative to its respective total input. Normal rabbit IgG was included as a negative control to verify the immunoprecipitation specificity (□). The results are presented as the mean ± S.E. of triplicate experiments.

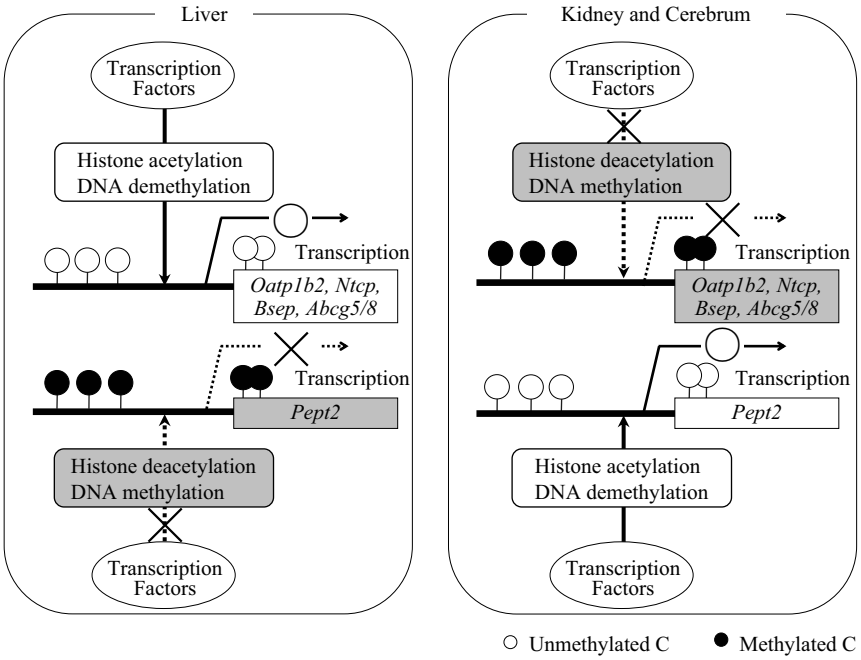

Fig. 5. Proposed mechanism underlying the transcriptional regulation of the tissue-specific transporters. DNA methylation neighboring the TSS evokes the condensed structure of chromatin through the deacetylation of histones, which interrupts the binding of transcription factors and consequently suppresses the expression of corresponding transporters in the tissue-specific manner.

References

Alrefai WA and Gill RK (2007) Bile acid transporters: structure, function, regulation and pathophysiological implications. *Pharmacol Res* **24:**1803–1823.

Ananthanarayanan M, Balasubramanian N, Makishima M, Mangelsdorf DJ, and Suchy FJ (2001) Human bile salt export pump promoter is transactivated by the farnesoid X receptor/bile acid receptor. *J Biol Chem* **276:**28857–28865.

Aoki M, Terada T, Kajiwara M, Ogasawara K, Ikai I, Ogawa O, Katsura T, and Inui K (2008) Kidney-specific expression of human organic cation transporter 2 (OCT2/SLC22A2) is regulated by DNA methylation. *Am J Physiol Renal Physiol* **295:** F165–F170.

Berge KE, Tian H, Graf GA, Yu L, Grishin NV, Schultz J, Kwiterovich P, Shan B, Barnes R, and Hobbs HH (2000) Accumulation of dietary cholesterol in sitosterolemia caused by mutations in adjacent ABC transporters. *Science* **290:**1771–1775.

Bird A (2002) DNA methylation patterns and epigenetic memory. *Genes Dev* **16:**6–21.

Borst P and Elferink RO (2002) Mammalian ABC transporters in health and disease. *Annu Rev Biochem* **71:**537–592.

Cereghini S (1996) Liver-enriched transcription factors and hepatocyte differentiation. *FASEB J* **10:**267–282.

Chandra P and Brouwer KL (2004) The complexities of hepatic drug transport: current knowledge and emerging concepts. *Pharmacol Res* **21:**719–735.

Eloranta JJ, Jung D, and Kullak-Ublick GA (2006) The human Na+-taurocholate cotransporting polypeptide gene is activated by glucocorticoid receptor and peroxisome proliferator-activated receptor-gamma coactivator-1alpha, and suppressed by bile acids via a small heterodimer partner-dependent mechanism. *Mol Endocrinol* **20:**65–79.

Evers R and Chu XY (2008) Role of the murine organic anion-transporting polypeptide 1b2 (Oatp1b2) in drug disposition and hepatotoxicity. *Mol Pharmacol* **74:**309–311.

Faber KN, Müller M, and Jansen PL (2003) Drug transport proteins in the liver. *Adv Drug Deliv Rev* **55:**107–124.

Fujii G, Nakamura Y, Tsukamoto D, Ito M, Shiba T, and Takamatsu N (2006) CpG methylation at the USF-binding site is important for the liver-specific transcription of the chipmunk HP-27 gene. *Biochem J* **395:**203–209.

Hagenbuch B and Meier PJ (2003) The superfamily of organic anion transporting polypeptides. *Biochim Biophys Acta* **1609:**1–18.

Hagenbuch B and Meier PJ (2004) Organic anion transporting polypeptides of the OATP/ SLC21 family: phylogenetic classification as OATP/ SLCO superfamily, new nomenclature and molecular/functional properties. *Pflugers Arch* **447:**653–665.

Hazard SE and Patel SB (2007) Sterolins ABCG5 and ABCG8: regulators of whole body dietary sterols. *Pflugers Arch* **453:**745–752.

Hediger MA, Romero MF, Peng JB, Rolfs A, Takanaga H, and Bruford EA (2004) The ABCs of solute carriers: physiological, pathological and therapeutic implications of human membrane transport proteins. Introduction. *Pflugers Arch* **447:**465–468.

Jung D, Hagenbuch B, Gresh L, Pontoglio M, Meier PJ, and Kullak-Ublick GA (2001) Characterization of the human OATP-C (SLC21A6) gene promoter and regulation of liver-specific OATP genes by hepatocyte nuclear factor 1α. *J Biol Chem* **276:**37206–37214.

Kidambi S and Patel SB (2008) Cholesterol and non-cholesterol sterol transporters: ABCG5, ABCG8 and NPC1L1: a review. *Xenobiotica* **38:**1119–1139.

Kikuchi R, Kusuhara H, Hattori N, Kim I, Shiota K, Gonzalez FJ, and Sugiyama Y (2007) Regulation of tissue-specific expression of the human and mouse urate transporter 1 gene by hepatocyte nuclear factor 1 α/β and DNA methylation. *Mol Pharmacol* **72:**1619–1625.

Kikuchi R, Kusuhara H, Hattori N, Shiota K, Kim I, Gonzalez FJ, and Sugiyama Y (2006) Regulation of the expression of human organic anion transporter 3 by hepatocyte nuclear factor α/β and DNA methylation. *Mol Pharmacol* **70:**887–896.

Kusuhara H and Sugiyama Y (2002) Role of transporters in the tissue-selective distribution and elimination of drugs: transporters in the liver, small intestine, brain and kidney. *J Control Release* **78:**43–54.

Lee MH, Lu K, Hazard S, Yu H, Shulenin S, Hidaka H, Kojima H, Allikmets R, Sakuma N, Pegoraro R, et al. (2001) Identification of a gene, ABCG5, important in the regulation of dietary cholesterol absorption. *Nat Genet* **27:**79–83.

Lu K, Lee MH, Hazard S, Brooks-Wilson A, Hidaka H, Kojima H, Ose L, Stalenhoef AF, Mietinnen T, Bjorkhem I, et al. (2001) Two genes that map to the STSL locus cause sitosterolemia: genomic structure and spectrum of mutations involving sterolin-1 and sterolin-2, encoded by ABCG5 and ABCG8, respectively. *Am J Hum Genet* **69:**278–290.

Maher JM, Slitt AL, Callaghan TN, Cheng X, Cheung C, Gonzalez FJ, and Klaassen CD (2006) Alterations in transporter expression in liver, kidney, and duodenum after targeted disruption of the transcription factor HNF1alpha. *Biochem Pharmacol* **72:**512–522.

Mita S, Suzuki H, Akita H, Hayashi H, Onuki R, Hofmann AF, and Sugiyama Y (2006) Vectorial transport of unconjugated and conjugated bile salts by monolayers of LLC-PK1 cells doubly transfected with human NTCP and BSEP or with rat Ntcp and Bsep. *Am J Physiol Gastrointest Liver Physiol* **290:**G550–G556.

Ohgane J, Yagi S, and Shiota K (2008) Epigenetics: the DNA methylation profile of tissue-dependent and differentially methylated regions in cells. *Placenta* **29 (Suppl A):**S29–S35.

Plass JR, Mol O, Heegsma J, Geuken M, Faber KN, Jansen PL, and Müller M (2002) Farnesoid X receptor and bile salts are involved in transcriptional regulation of the gene encoding the human bile salt export pump. *Hepatology* **35:**589–596.

Shiota K (2004) DNA methylation profiles of CpG islands for cellular differentiation and development in mammals. *Cytogenet Genome Res* **105:**325–334.

Shitara Y, Horie T, and Sugiyama Y (2006) Transporters as a determinant of drug clearance and tissue distribution. *Eur J Pharm Sci* **27:**425–446.

Sinal CJ, Tohkin M, Miyata M, Ward JM, Lambert G, and Gonzalez FJ (2000) Targeted disruption of the nuclear receptor FXR/BAR impairs bile acid and lipid homeostasis. *Cell* **102:**731–744.

Stefková J, Poledne R, and Hubácek JA (2004) ATP-binding cassette (ABC) transporters in human metabolism and diseases. *Physiol Res* **53:**235–243.

Strautnieks SS, Bull LN, Knisely AS, Kocoshis SA, Dahl N, Arnell H, Sokal E, Dahan K, Childs S, Ling V, et al. (1998) A gene encoding a liver-specific ABC transporter is mutated in progressive familial intrahepatic cholestasis. *Nat Genet* **20:**233–238.

Sumi K, Tanaka T, Uchida A, Magoori K, Urashima Y, Ohashi R, Ohguchi H, Okamura M, Kudo H, Daigo K, et al. (2007) Cooperative interaction between hepatocyte nuclear factor 4 alpha and GATA transcription factors regulates ATP-binding cassette sterol transporters ABCG5 and ABCG8. *Mol Cell Biol* **27:**4248–4260.

Tohyama K, Kusuhara H, and Sugiyama Y (2004) Involvement of multispecific organic anion transporter, Oatp14 (Slc21a14), in the transport of thyroxine across the blood-brain barrier. *Endocrinology* **145:**4384–4391.

Trauner M and Boyer JL (2003) Bile salt transporters: molecular characterization, function, and regulation. *Physiol Rev* **83:**633–671.

Wolkoff AW and Cohen DE (2003) Bile acid regulation of hepatic physiology: I. Hepatocyte transport of bile acids. *Am J Physiol Gastrointest Liver Physiol* **284:** G175–G179.

Yagi S, Hirabayashi K, Sato S, Li W, Takahashi Y, Hirakawa T, Wu G, Hattori N, Hattori N, Ohgane J, et al. (2008) DNA methylation profile of tissue-dependent and differentially methylated regions (T-DMRs) in mouse promoter regions demonstrating tissue-specific gene expression. *Genome Res* **18:**1969–1978.

Address correspondence to: Dr. Yuichi Sugiyama, Department of Molecular Pharmacokinetics, Graduate School of Pharmaceutical Sciences, The University of Tokyo, 7-3-1 Hongo, Bunkyo-ku, Tokyo 113-0033, Japan. E-Mail: sugiyama@mol.f.u-tokyo.ac.jp